EphA2 and Ephrin-A5 Guide Eye Lens Suture Alignment and Influence Whole Lens Resilience

Catherine Cheng

School of Optometry and Vision Science Program, Indiana University, Bloomington, Indiana, United States

Correspondence: Catherine Cheng, School of Optometry and Vision Science Program, Indiana University, 800 E. Atwater Avenue, Bloomington, IN 47405, USA; ckcheng@iu.edu.

Received: July 20, 2021
Accepted: October 12, 2021
Published: December 2, 2021

Citation: Cheng C. EphA2 and ephrin-A5 guide eye lens suture alignment and influence whole lens resilience. *Invest Ophthalmol Vis Sci.* 2021;62(15):3. https://doi.org/10.1167/iovs.62.15.3

Purpose. Fine focusing of light by the eye lens onto the retina relies on the ability of the lens to change shape during the process of accommodation. Little is known about the cellular structures that regulate elasticity and resilience. We tested whether Eph–ephrin signaling is involved in lens biomechanical properties.

Methods. We used confocal microscopy and tissue mechanical testing to examine mouse lenses with genetic disruption of EphA2 or ephrin-A5.

Results. Confocal imaging revealed misalignment of the suture between each shell of newly added fiber cells in knockout lenses. Despite having disordered sutures, loss of EphA2 or ephrin-A5 did not affect lens stiffness. Surprisingly, knockout lenses were more resilient and recovered almost completely after load removal. Confocal microscopy and quantitative image analysis from live lenses before, during, and after compression revealed that knockout lenses had misaligned Y-sutures, leading to a change in force distribution during compression. Knockout lenses displayed decreased separation of fiber cell tips at the anterior suture at high loads and had more complete recovery after load removal, which leads to improved whole-lens resiliency.

Conclusions. EphA2 and ephrin-A5 are needed for normal patterning of fiber cell tips and the formation of a well-aligned Y-suture with fiber tips stacked on top of previous generations of fiber cells. The misalignment of lens sutures leads to increased resilience after compression. The data suggest that alignment of the Y-suture may constrain the overall elasticity and resilience of the lens.

Keywords: biomechanics, fiber cells, compression, elasticity, live lens imaging

The eye lens is an avascular, transparent, highly refractive, and biconvex structure that focuses light from objects onto the retina, and the function of the lens is intimately tied to its shape, biomechanical properties, transparency, and refractive index. The lens changes shape in a process known as accommodation to focus light from near objects, and the transition between distance and near focusing is seamless and instantaneous in young people. Accommodation requires the lens to be pliable and elastic to flatten for distance vision and to return to resting spherical shape for near vision. With age, presbyopia is caused by a reduction in the ability of the lens to change shape during focusing (accommodation) and, by extension, the need for reading glasses.[1–3] Although it has long been hypothesized that age-related increases in lens stiffness are linked to presbyopia,[1–6] little is known about the cellular and molecular mechanisms that determine overall lens tissue stiffness and resilience.

The lens consists of a monolayer of anterior epithelial cells and elongated fiber cells enclosed by the lens capsule. Lifelong lens growth relies on epithelial cell proliferation, differentiation, and elongation into secondary fibers at the lens equator to surround previous generations of fibers.[7] Fiber cell tips stretch from the anterior to posterior poles and form Y-shaped sutures directly below the anterior epithelial cells and above the posterior capsule.[8,9] In contrast to Y-shaped sutures in rodent lenses, human lenses develop highly branched sutures as the lens grows with age.[10,11] Fiber cells, hexagon-shaped in cross-section, are packed tightly to minimize intercellular space and light scattering.[9]

Our recent work has demonstrated that abnormal actin networks can lead to changes in lens stiffness.[12,13] Loss of actin-binding proteins can lead to changes in fiber cell interdigitation or rearrangement of the actin filament networks to cause decreased lens stiffness at low or high compressive loads, respectively. Other reports have shown that loss of cytoskeletal components, such as specialized beaded intermediate filament proteins, filensin and CP49,[14,15] membrane skeleton proteins periaxin and ankyrin-B,[16] and water channel aquaporin 0[17] from the lens membrane can lead to abnormal fiber cells, lens growth defects, and decreased lens stiffness. Our results from compression of wild-type (WT) mouse lenses revealed that the resilience, or recovery of the lens after removal of load, depends on the closure of the Y-suture that opens under compression.[18]

Bidirectional signaling mediated by Eph receptor tyrosine kinases and membrane-anchored ephrins is a major form of cell–cell contact-dependent communication that plays a part in the important functions in a broad range of cell–cell recognition events, including axon pathfinding, early segmentation and organ morphogenesis, and

cytoskeletal dynamics.[19–23] Recent studies, including our work, have reported that the loss of EphA2 or ephrin-A5 in the lens can result in abnormal actin cytoskeleton and fiber cell morphologies. In mice, loss of EphA2 is associated with disruption of the actin cytoskeleton, cell shape, and organization of equatorial epithelial cells,[24] as well as with misaligned and disorganized fiber cells.[24–28] Our work showed that EphA2 signals through Src and cortactin to recruit actin to the vertices of hexagonal equatorial epithelial cells, controlling organization of meridional rows and fiber cells.[24] The *ephrin-A5* knockout ($^{-/-}$ or KO) lenses develop cataracts of varying severity depending on strain background.[25,29,30] In the C57BL6 background, *ephrin-A5*$^{-/-}$ lenses often develop anterior cataracts caused by abnormal localization of E-cadherin and β-catenin along with epithelial–mesenchymal transition and aberrant expression of α-smooth muscle actin in KO anterior epithelial cells.[25] In contrast, mixed background (129/SV/C57BL6) *ephrin-A5*$^{-/-}$ mice displayed severe fiber cell degeneration and lens rupture.[29–31]

We have examined fiber cells in live *ephrin-A5*$^{-/-}$ and *EphA2*$^{-/-}$ lenses using confocal microscopy, and the data reveal that KO lenses have a misaligned lens suture apex between different shells of fiber cells. We have found that the biomechanical properties of *ephrin-A5*$^{-/-}$ and *EphA2*$^{-/-}$ lenses were affected by changes in the lens suture patterning. There is no difference in the overall stiffness of *ephrin-A5*$^{-/-}$ and *EphA2*$^{-/-}$ lenses compared with controls, but there is an unexpected increase in resilience of KO lenses. Misalignment of KO lens sutures leads to a change in force transmission and more complete recovery of the KO lenses after compressive load removal. These data indicate that EphA2 and ephrin-A5 may interact at the tips of lens fiber cells to enable precise lens suture patterning. This is the first work to demonstrate that lens resilience can be affected by suture geometry and that Eph–ephrin signaling plays a role in suture alignment and patterning.

Material and Methods

Mice

Mice were maintained in accordance with an approved animal protocol (Indiana University Bloomington Institutional Animal Care and Use Committee) and the ARVO Statement for the Use of Animals in Ophthalmic and Vision Research. All mice were maintained in the C57BL/6J background with wild-type *Bfsp2* (CP49) genes. Genotyping was performed by automated quantitative PCR on toe or tail snips (Transnetyx, Cordova, TN, USA). Male and female littermates were used for experiments.

The *ephrin-A5*$^{-/-}$ and *EphA2*$^{-/-}$ mice were generated and maintained as previously described.[24,25,32,33] Rosa26-tdTomato tandem dimer-Tomato (B6.129(Cg)-Gt(ROSA) (tdTomato) (The Jackson Laboratory, Bar Harbor, ME, USA) mice express tdTomato protein fused in frame to connexin 43.[34] We previously showed that tdTomato expression was present at the plasma membranes of lens epithelial and fiber cells.[18] WT and KO knockout mice with one copy of the tdTomato transgene were generated by intercrossing tdTomato+ WT mice with *ephrin-A5*$^{-/-}$ or *EphA2*$^{-/-}$ mice and then intercrossing tdTomato+ heterozygous offspring with non-tdTomato+ heterozygous offspring. Because *ephrin-A5*$^{-/-}$ lenses sometimes develop obvious anterior cataracts that interfere with the suture region,[25] we excluded those lenses from the present study.

Lens Biomechanical Testing

We tested the stiffness of lenses from 8-week-old *ephrin-A5*$^{+/+}$, *ephrin-A5*$^{-/-}$, *EphA2*$^{+/+}$, and *EphA2*$^{-/-}$ mice using sequential application of glass coverslips as previously described.[15,35,36] Briefly, freshly dissected lenses were imaged and compressed in a custom chamber filled with 1× PBS (14190; Thermo Fisher Scientific, Waltham, MA, USA). We did not observe any obvious changes in lens transparency during the duration of the experiments. Glass coverslips were loaded onto the lens one at a time, and images of the lens before, during, and after were captured by an Olympus SZ-11 dissecting microscope with digital camera (Olympus Corporation, Tokyo, Japan) or a Zeiss SteREO Discovery V8 microscope with Axiocam 305 Color camera (Carl Zeiss Microscopy, Jena, Germany). ImageJ (National Institutes of Health, Bethesda, MD, USA) was used to perform measurements to calculate strain: $\varepsilon = (d - d_0)/d_0$, where ε is strain, d is the axial or equatorial diameter at a given load, and d_0 is the corresponding axial or equatorial diameter at zero load. Images before and after compression were used to calculate resilience as the ratio between the pre-compression axial diameter over the post-compression axial diameter. Strain curves and resilience were calculated in Excel (Microsoft Corporation, Redmond, WA, USA) and plotted in Prism 9.2 (GraphPad Software, San Diego, CA, USA). Plots represent mean ± SD. Student's *t*-test (two-tailed) was used to determine statistical significance.

Compression of Live Lenses Under a Confocal Microscope

Confocal examination of lens anterior regions under compression was performed on live, partially dissected lenses from 8-week-old tdTomato+ *ephrin-A5*$^{+/+}$, *ephrin-A5*$^{-/-}$, *EphA2*$^{+/+}$, and *EphA2*$^{-/-}$ lenses. Partial dissection of lenses was performed as previously described to minimize damage that can occur in the anterior region due to complete lens dissection from the globe.[18] Briefly, a sharp scalpel was used to make a small incision at the corneoscleral junction, and the cornea and iris were carefully removed by microdissection scissors and tweezers. Next, the optic nerve and half of the posterior eyecup were cut away circumferentially around the eye equator, exposing the posterior regions of the lens. The lens was left with a band of eyecup tissue around the equator.

Imaging and staining of live lenses were performed as previously described.[18,37] Briefly, to visualize the epithelial cell nuclei, partially dissected lenses were stained with Hoechst 33342 (1:500; Biotium, Fremont, CA, USA) in PBS (137-mM NaCl, 2.7-mM KCl, 8.1-mM Na_2HPO_4, and 1.5-mM KH_2PO_4, pH 8.1) for 15 minutes at room temperature with gentle shaking. Live lenses were then imaged in a glass-bottomed tissue culture dish (FluoroDish; World Precision Instruments, Sarasota, FL, USA) in 3 mL of PBS supplemented with 1.8 units of Oxyrase (Oxyrase, Inc., Mansfield, OH, USA). Coverslips were applied to lenses, and z-stacks of the lens anterior were collected before, during, and after compression using a Zeiss LSM 800 confocal microscope with a 10× objective (0.6× zoom with Z step of 2 µm and 65 steps).

Confocal Image Analysis

Similar to our previous study,[18] suture gap measurements were made using Zeiss ZEN software by manually outlining suture maximum-intensity projection images of z-stacks through the anterior 130 µm of tdTomato+ lenses. We compared the suture in lenses prior to, under maximum compression (~29% strain), and after load removal. Because the sutures are quite variable in shape and branches, even between control lenses from the same mouse, we calculated and plotted the suture gap area under compression and after compression as a percentage of the pre-compression suture gap area. We also used pre-compression z-stacks to determine the pattern of suture branches in different layers of WT and KO lenses.

Results

Suture Tips Were Misaligned Between Shells of Fibers in *EphA2*$^{-/-}$ and *Ephrin-A5*$^{-/-}$ Lenses

We conducted a detailed examination of fiber cells by confocal imaging of live tdTomato+ control and KO lenses. We observed that KO lenses often displayed irregular anterior Y-sutures. In control lenses, the Y-suture had a fixed apex that was in the same location through the many shells of elongating lens fibers (Figs. 1A, 1B; top rows, red asterisks). The steady localization of the apex of the anterior suture can be viewed in Supplementary Videos S1 and S2, which show movies of the confocal z-stacks through the anterior of control lenses. In contrast, KO lenses often displayed changes in the location of the suture apex between different shells of fiber cells (Figs. 1A, 1B; middle rows; red, yellow, and green asterisks). The apex of the KO sutures traveled in all directions between different layers of lens fibers (Fig. 2, asterisks and arrows; Supplementary Videos S3 and S4). This defect was observed in 11 of 13 *EphA2*$^{-/-}$ lenses and 11 of 14 *ephrin-A5*$^{-/-}$ lenses; it was seen in just one of 15 *EphA2*$^{+/+}$ lenses and in none of the 12 *ephrin-A5*$^{+/+}$ lenses that were imaged. Magnified images of the suture region revealed distinct divisions between fiber cell bundles resulting in distinct boundaries between the branches of the suture in the control lenses (Figs. 2A, 2B; top rows). Although the suture apex drifted in the *EphA2*$^{-/-}$ lens, the branches of the suture had a distinct boundary (Fig. 2B, bottom row). However, in the *ephrin-A5*$^{-/-}$ lens, the fiber cell tips did not form clear boundaries between neighboring cells, resulting in indistinct boundaries (Fig. 2A, arrowheads).

In addition to the suture apex changes, we also commonly observed additional branches in sutures of KO lenses (Figs. 1A, 1B; bottom rows, arrows). The extra branches were often present in the outer layers of newly added lens fibers (Supplementary Videos S5 and S6). We found additional suture branches in 7 of 13 *EphA2*$^{-/-}$ lenses and 11 of 14 *ephrin-A5*$^{-/-}$ lenses. In agreement with our previous data in WT lenses,[18] we also observed these branching defects in four of 15 *EphA2*$^{+/+}$ lenses and in five of 12 *ephrin-A5*$^{+/+}$ lenses. Although KO lenses have more variable suture branches, the WT lenses also had this defect, albeit in fewer lenses. We observed that *EphA2*$^{+/+}$ and *ephrin-A5*$^{+/+}$ lenses had normal Y-sutures, and a few lenses had four-pronged sutures in the outer layers that returned to a normal Y-suture in inner layers. In *EphA2*$^{-/-}$ lenses, we found a variety of suture branching changes with four-pronged sutures, Y-sutures, and line (two-pronged) sutures. Most *EphA2*$^{-/-}$ lenses had a normal Y-suture in deeper fiber cell layers. The *ephrin-A5*$^{-/-}$ lenses had the most complex suture branches with up to six prongs and as few as two prongs. About half of *ephrin-A5*$^{-/-}$ lenses had a normal Y-suture in deeper fiber cell layers.

EphA2$^{-/-}$ and *Ephrin-A5*$^{-/-}$ Lenses Displayed Increased Resilience After Biomechanical Testing

To determine whether disruption of suture alignment affects biomechanical properties, we used our simple coverslip application assay to determine lens stiffness under compression.[35] We calculated axial and equatorial compressive strain, a dimensionless measurement of percent change in the lens diameter and recovery after load removal (resilience), by comparing the pre- and post-loading axial diameter of the lens. We did not find any change in stiffness among the 8-week-old control, *ephrin-A5*$^{-/-}$, and *EphA2*$^{-/-}$ lenses (Fig. 3, left and middle columns), but, surprisingly, the loss of either EphA2 or ephrin-A5 led to increased resilience (Fig. 3, right column), suggesting that Eph–ephrin signaling affects lens elasticity.

Although the resilience of lenses was increased after the maximum compressive load (29% strain) in KO lenses, we further analyzed whether resilience differences between control and KO lenses were present after lower compressive loads (14% or 23% strain). After 14% strain, the resilience of control and KO lenses was over 99%, and there was no difference between control and KO lenses (Supplementary Fig. S1, left column). Similarly, after 23% strain, control and KO lenses recovered to ~98% without significant difference between control and KO samples (Supplementary Fig. S1, right column). These resilience numbers are consistent with our previous work on WT lenses.[18]

Under Compression, the Anterior Suture of *EphA2*$^{-/-}$ and *Ephrin-A5*$^{-/-}$ Lenses Recovered More Fully After Load Removal

Our previous work demonstrated that mouse lens resilience is affected by suture recovery after load removal and that incomplete closure of the suture gap after compression led to decreased lens resilience.[18] The unexpected increase in the resilience of KO lenses after max compressive load led us to examine the anterior suture more carefully in live lenses. Z-stacks through the anterior region of tdTomato+ control and KO lens were analyzed to determine the suture gap area before, during maximum compression at 29% strain, and after load removal. Representative images of the suture gap area revealed that both control and KO lenses had increased suture gap area under compression and recovered after load removal (Figs. 4A, 4C). Quantification of the suture gap area as a percent of the pre-compression suture gap area revealed that the suture gap area was smaller in KO versus control lenses under compression and after compression after load removal (Figs. 4B, 4D). The decreased enlargement of the suture gap area under compression and the increased closure of the suture gap area after load removal in KO lenses led to increased resilience.

Investigative Ophthalmology & Visual Science

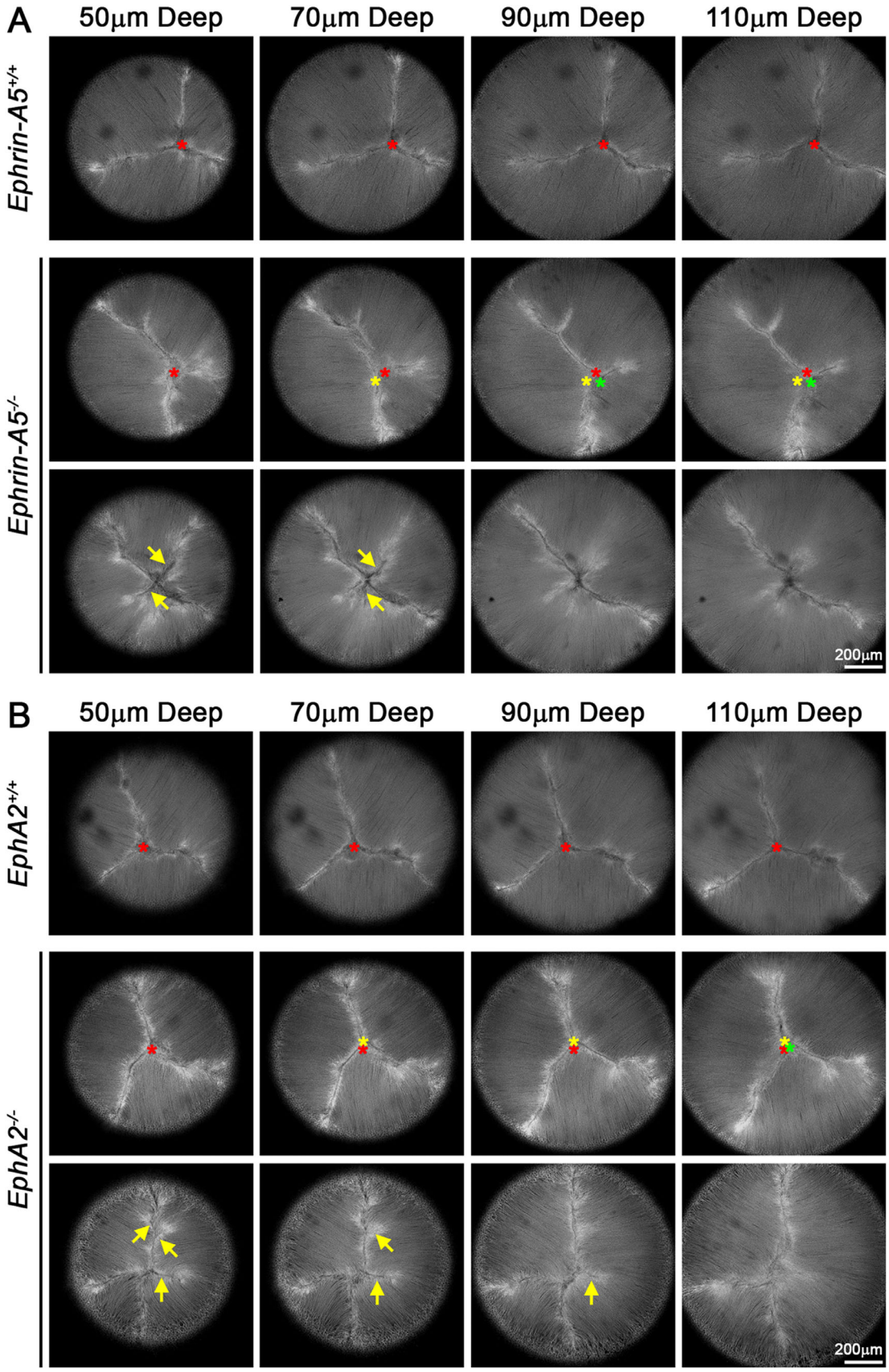

Figure 1. Single optical images through the anterior of the lens revealed abnormal suture apex localization and increased suture branching in *ephrin-A5*$^{-/-}$ and *EphA2*$^{-/-}$ lenses. (**A**) Images of the lens suture at various depths (50–110 µm) from the anterior pole from representative lenses showed that the control lens had a normal Y-shaped suture and that the suture apex (marked with a *red asterisk*) remained in the same location between shells of fiber cells. In contrast, in the *ephrin-A5*$^{-/-}$ lens (*middle row*), the suture apex changed location between shells of lens fibers (*red*, *yellow*, and *green asterisks*). The KO lens also showed extra branches in the Y-suture in the outer layers of the lens (*arrows*) that disappeared in deeper fiber layers. (**B**) Similar to *ephrin-A5*$^{-/-}$ lenses, *EphA2*$^{-/-}$ lenses also displayed wandering suture apex locations between shells of fiber cells (*red*, *yellow*, and *green asterisks*) and often displayed extra branches in newly differentiating layers of lens fibers (*arrows*). *Scale bars*: 200 µm.

Investigative Ophthalmology & Visual Science

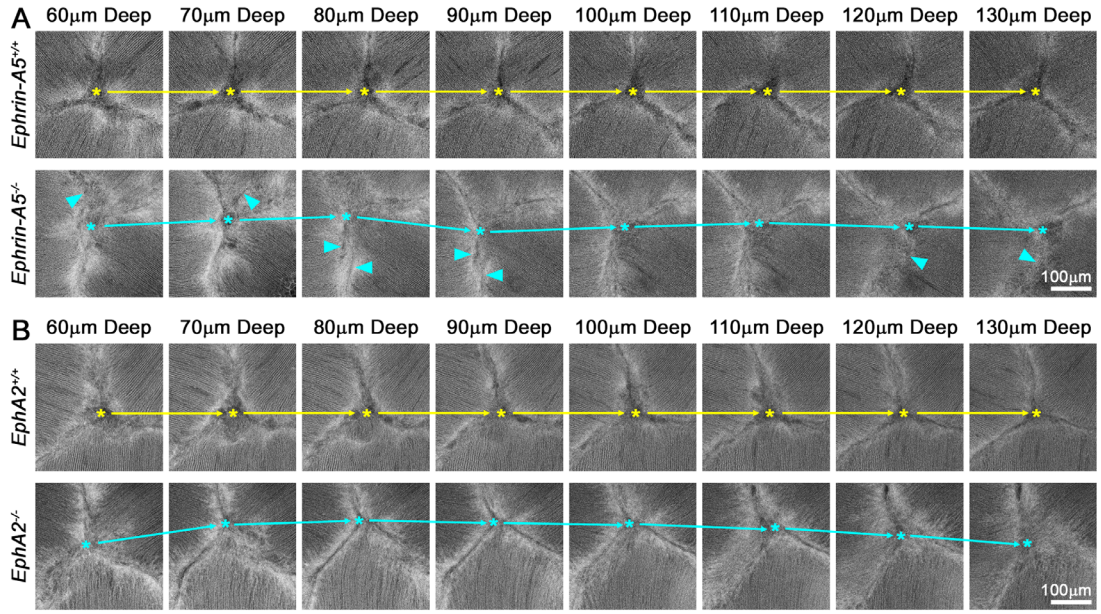

Figure 2. Magnified single optical images of the anterior suture region showed the misalignment of the suture apex in *ephrin-A5*$^{-/-}$ and *EphA2*$^{-/-}$ lenses. (**A**) Images of the center of the lens suture at various depths (60–130 µm) from the anterior pole. *Asterisks* mark the apex of the lens suture, and *arrows* highlight the movement of the apex in the *ephrin-A5*$^{-/-}$ lens compared with the control lens. The suture branches of the *ephrin-A5*$^{-/-}$ lens were often indistinct (*arrowheads*), indicating that fiber cells tips were also misaligned. (**B**) In the *EphA2*$^{-/-}$ lens, the suture apex was misaligned and moved significantly between layers. The suture branches in the *EphA2*$^{-/-}$ lens were distinct, like the control lens. *Scale bars*: 100 µm.

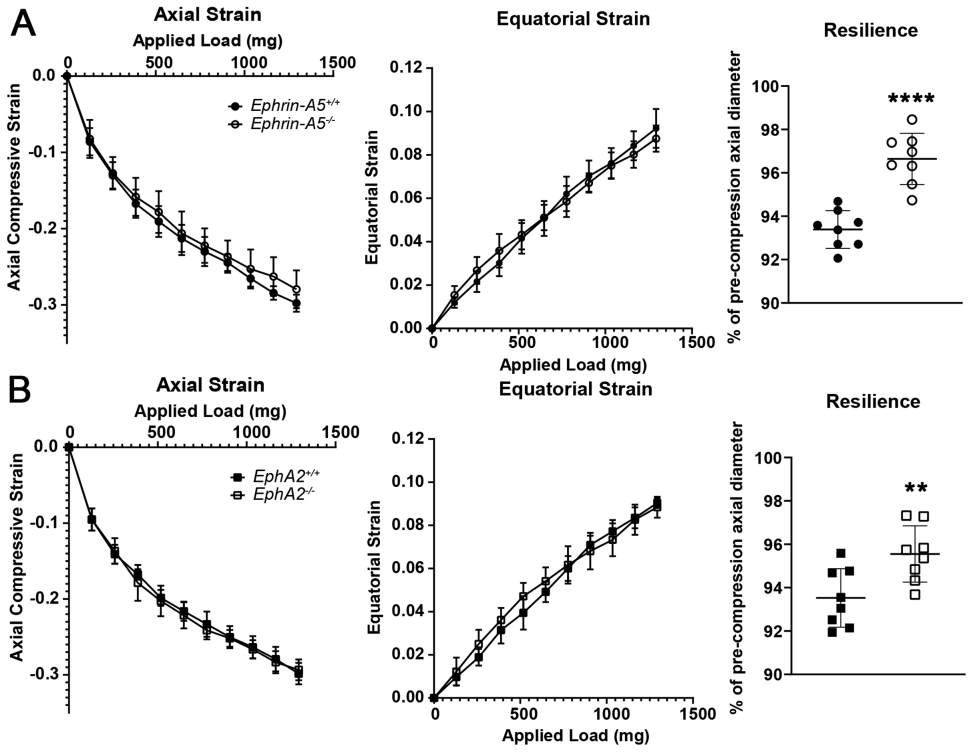

Figure 3. *EphA2*$^{-/-}$ and *ephrin-A5*$^{-/-}$ lenses displayed increased resilience after compression. (**A**) Compression testing of 8-week-old *ephrin-A5*$^{+/+}$ and *ephrin-A5*$^{-/-}$ lenses revealed no differences in lens stiffness (axial compression and equatorial expansion strains). The *ephrin-A5*$^{-/-}$ lenses had increased resilience, calculated as the ratio of the post-compression over pre-compression axial diameter. KO lenses recovered to 96.64% ± 1.18% of the pre-compression axial diameter, whereas control lenses recovered to 93.39% ± 0.87% of the pre-loading axial diameter. (**B**) Similarly, although there was no change in lens stiffness between *EphA2*$^{+/+}$ and *EphA2*$^{-/-}$ lenses, the KO lenses recovered to 95.55% ± 1.30% of the pre-compression axial diameter compared with 93.53% ± 1.35% of the pre-loading axial diameter in littermate controls ($n = 8$ lenses for each genotype). $^{**}P < 0.01$; $^{****}P < 0.0001$.

Investigative Ophthalmology & Visual Science

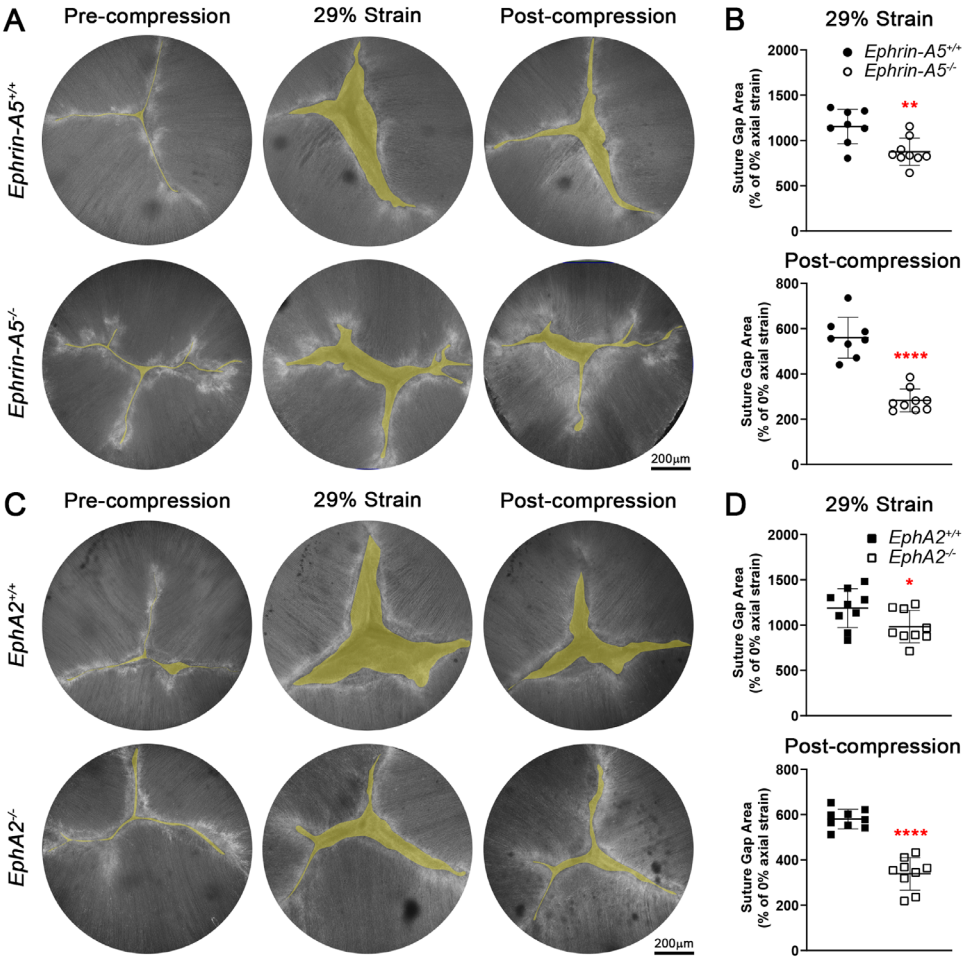

Figure 4. Under maximum compressive load and post-compression, the suture gap area was smaller in *ephrin-A5*$^{-/-}$ and *EphA2*$^{-/-}$ lenses. (**A**) Maximum-intensity projections of the z-stack through the anterior 130 µm of representative lenses before, during, and after compression. *Yellow overlays* outline the suture gap area. In *ephrin-A5*$^{-/-}$ lenses, the suture gap appeared smaller at 29% strain (maximum compression) and post-compression after load removal. (**B**) Quantification of the suture gap area revealed a statistically significant decrease in suture gap area of the *ephrin-A5*$^{-/-}$ lenses under 29% strain and after compression. (**C**, **D**) Similar decreases in suture gap area of *EphA2*$^{-/-}$ lenses can be observed in representative images and through area quantification ($n = 8$ or 9 lenses for each genotype). *$P < 0.05$; **$P < 0.01$; ****$P < 0.0001$. *Scale bars*: 200 µm.

Discussion

Our data show that, although EphA2 and ephrin-A5 did not play a role in lens stiffness, the loss of either protein led to changes in suture alignment between shells of the lens fibers, and the change in the lens suture apex positioning led to increased resilience of KO lenses after compressive load removal (Fig. 5). Under compression, the suture gap in KO lenses did not expand as much as that in control lenses, and after load removal the suture gap recovered more completely in KO lenses. These results are the first to demonstrate that lens suture patterning and alignment directly influence lens resilience. This work further confirms our hypothesis that hexagonal cell shape and ordered packing of lens fibers cells are not required for lens biomechanical properties. We had previously observed that, even though lenses from very old mice had misaligned and misshapen lens fibers, those lenses continued to increase in stiffness.[37] *EphA2*$^{-/-}$ lenses display obvious fiber cell packing defects[24–28] due to misalignment and lack of the normal hexagonal shape of equatorial lens epithelial cells before fiber cell differentiation.[24] But, this misalignment of the fibers and change in cell shape do not affect lens stiffness.

Little is known about lens resilience and the cell structures that affect lens elasticity. Consistent with previous observations in WT lenses,[18] we find that control and KO lenses under low compressive force (14% strain) recovered completely after load removal. However, under high compressive loads (29% strain), the suture gap in WT lenses opened and did not recover completely, leading to ~94% recovery of the pre-loading state.[18,37] Our work on actin-binding proteins revealed that changes in the F-actin network due to disruption of an actin-stabilizing protein, tropomyosin 3.5, led to decreased lens stiffness and resilience.[12] In that mouse model, the decrease in lens resilience is most likely a result of the significantly decreased lens stiffness. There are conflicting reports about the role of CP49, a component of lens beaded intermediate filaments, in lens resilience. One study showed that loss of CP49 leads to decreased lens stiffness but increased lens resilience.[14] However, another report found no change in resilience in lenses without CP49.[15] These two studies used

different instruments and compression protocols to measure lens resilience, which may be the reason for the conflicting results. Based on re-analysis of the coverslip compression data for CP49 control and KO lenses from Gokhin et al.,[15] no impact of CP49 deletion on lens resilience was observed (data not shown). Our data from *EphA2*$^{-/-}$ and *ephrin-A5*$^{-/-}$ lenses showed that KO lenses had normal lens stiffness but increased resilience, likely due to misalignment of the suture apex between different layers of lens fiber cells. This change in apex location affects force transmission through the tissue during compression. The suture opens under compression, but the gap is smaller in KO lenses than in control lenses. After load removal, the smaller suture gap in KO lenses closes more completely, leading to increased resilience. Our results indicate that Eph–ephrin signaling may not directly affect lens biomechanical properties, but the change in KO lens resilience suggests that the alignment of the Y-suture constrains lens elasticity and resilience.

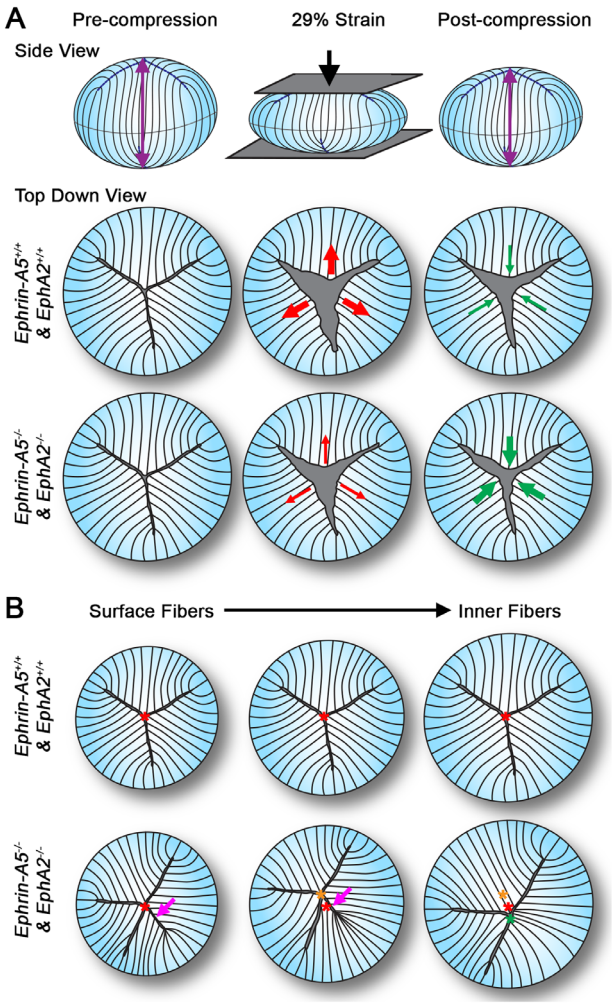

Figure 5. (**A**) Our data show that, under compressive load, *ephrin-A5*$^{-/-}$ and *EphA2*$^{-/-}$ lenses had smaller suture gap areas, and after loading these KO lenses had better recovery and closure of the lens suture gap, leading to increased lens resilience. (**B**) Compared with control lenses, the *ephrin-A5*$^{-/-}$ and *EphA2*$^{-/-}$ lenses had misaligned suture apex locations between fiber shells, and *ephrin-A5*$^{-/-}$ and *EphA2*$^{-/-}$ lenses often had extra branches of the lens suture present in the surface (outer) layers of lens fibers. These extra branches often disappeared in deeper (inner) fiber layers. The branching defect was also present in some control lenses, but the control lenses did not display the suture apex misalignment defect. Illustration not drawn to scale.

The suture branching data from the control lenses matches our previous observations that some control lenses have branched sutures with more than the standard three prongs,[18] and the branching defect in KO lenses was similar to that of a prior report.[28] Non-accommodating WT mouse lenses generally have Y-shaped sutures with three branches, and some lenses display four branches based on data in this work and our previous results.[18] In WT mouse lenses, we observe that the Y-suture was continuous between the shells of secondary fiber cells. In contrast, in accommodating human lenses, the suture is Y-shaped in embryonic lenses and quickly adds more branches to become star-shaped in infancy. With age, adult human lenses have complex sutures with 2°, 3°, and 4° branches. In primate lenses, the suture is offset between successive growth shells of fiber cells, forming a discontinuous suture.[10,11] The *EphA2*$^{-/-}$ and *ephrin-A5*$^{-/-}$ mouse lenses mimic human lens branching patterns, with the outermost layers of the lens adding additional branches, sometimes beyond four prongs, and the offset suture apex between shells of fibers, leading to increased lens resilience. More work should be done to determine how the geometric patterning of fiber cells and sutures could also play a significant role in determining lens resilience in non-accommodating and accommodating lenses.

Due to the suture branching changes being present in a significant number of control lenses and similar changes being seen in the *EphA2*$^{-/-}$ lenses, it is unlikely that branching patterns heavily influence mouse lens resilience or that the branching pattern of the suture is only controlled by EphA2 or ephrin-A5. Rather, it is more likely that EphA2 and ephrin-A5 influence branching patterns by affecting the suture apex location. We hypothesize that the loss of ephrin-A5 affects suture branching more than the loss of EphA2 due to changes that are present in the *ephrin-A5*$^{-/-}$ anterior epithelial cells.[25] The *ephrin-A5*$^{-/-}$ anterior epithelial cells have abnormal cell–cell adhesions,[25] and these changes likely affect the connection between fiber cell tips and the apical surface of anterior epithelial cells during fiber cell migration, possibly leading to changes in suture branching patterns. Based on this and previous works, there may be multiple factors that affect resilience after compression, including the arrangement of lens fibers at the suture, as well as cell–cell adhesion and cytoskeletal components of lens epithelial and fiber cells.

Our previous work in young 3-week-old lenses did not reveal these suture defects for several reasons.[25,38] We utilized a ubiquitously expressed green fluorescent protein (GFP) transgene as the way to visualize live lenses. Although we could see the apex of the suture in most cases, it was not a feature that could be easily distinguished in the fiber cell layers because the GFP signal was uniformly distributed between fibers. Thus, in most cases we could see the Y-suture in the KO lenses, but the branches and misalignment of the suture apex were not apparent. From the data in this work, we noticed that the branching defect was more obvious in the newly formed layers of lens fibers closer to the outermost regions of the lens. This indicates that these layers were added as the animals aged, and we have utilized 8-week-old animals in this study compared to 3-week-old animals in the previous study. It is important to keep these

Investigative Ophthalmology & Visual Science

factors in mind when comparing data between different studies of the same animal models.

In *ephrin-A5*$^{-/-}$ lenses, a normal hexagonal cell shape and organized packing of lens fibers can be seen.[25,38] Despite the normal packing and shape of lens fibers, the suture apex is misaligned in *ephrin-A5*$^{-/-}$ lenses. These data suggest that the mechanism for fiber cell shape and packing, which requires EphA2 and Src signaling to affect the actin cytoskeleton,[24] does not control the migration of lens fiber cell tips toward the anterior/posterior pole. There is another signaling mechanism through EphA2 and/or ephrin-A5 to guide suture apex localization and alignment between fiber cell layers. Eph–ephrin bidirectional signaling has been shown in other systems, including the retina, to have an important role in cell patterning, migration, and attraction and repulsion by regulating the cytoskeleton (reviewed in Lisabeth et al.[39] and Pasquale[40]). In the retina, brain, and other somatosensory systems, attraction and repulsion mediated by gradients of Ephs and ephrins, including ephrin-A5, are responsible for normal pattering of axons to determine unique synaptic targets.[41–44] Signaling through EphA2 and ephrin-A5 could provide cues for elongating fiber cell tips to detach from the apical surface of anterior epithelial cells or the posterior lens capsule to contact neighboring fibers to form the lens suture. It is not clear at this time whether this signaling is through interactions between EphA2 and ephrin-A5 or if there are other ephrin ligands or Eph receptors required for formation of the normal lens suture. Due to the promiscuous nature of Eph–ephrin interactions, each ligand and receptor may have multiple partners,[39,45,46] and this greatly complicates the identification of the cogent partners for EphA2 and ephrin-A5 in the lens. We previously suggested that EphA2 and ephrin-A5 are not a receptor–ligand pair in the lens based on double KO studies looking at the epithelial cell defects and cataract phenotypes.[38] Although *EphA2*$^{-/-}$ and *ephrin-A5*$^{-/-}$ lenses display misalignment of the suture apex, the defect in *ephrin-A5*$^{-/-}$ lenses is more complex, with indistinct suture branches and misalignment of the lens fiber tips. It appears possible that EphA2 and ephrin-A5 only interact in a specific subpopulation of lens cells at the suture apex based on the shared suture apex misalignment phenotype between the two KO mouse lines, but ephrin-A5 may have a different partner receptor that is required for alignment of the fiber cell tips along the suture branches. It remains to be determined whether EphA2 and ephrin-A5 interact at the fiber cell tips between neighboring cells and/or between fiber cells and anterior epithelial cells. This will require further studies to reveal other Ephs and ephrins in the lens and development of an effective method to immunolabel proteins at fiber cell tips in the lens suture.

Acknowledgments

The author thanks Bradley A. Spicer, Aalaa Shahin, Jackson T. Clark, and Jessica Palmer for assistance with the live lens confocal imaging and appreciates the technical assistance of Subashree Murugan and Michael Vu with lens resilience tests. The author also thanks David Gokhin, PhD, for sharing the coverslip compression testing data from CP49 control and knockout lenses and Justin Parreno, PhD, and Matthew A. Reilly, PhD, for their critical reading of the manuscript and helpful discussion.

Supported by a grant from the National Eye Institute, National Institutes of Health (R01 EY032056 to CC).

Disclosure: **C. Cheng**, None

References

1. Heys KR, Cram SL, Truscott RJ. Massive increase in the stiffness of the human lens nucleus with age: the basis for presbyopia? *Mol Vis*. 2004;10:956–963.
2. Glasser A, Campbell MC. Biometric, optical and physical changes in the isolated human crystalline lens with age in relation to presbyopia. *Vision Res*. 1999;39:1991–2015.
3. Weeber HA, Eckert G, Soergel F, Meyer CH, Pechhold W, van der Heijde RG. Dynamic mechanical properties of human lenses. *Exp Eye Res*. 2005;80:425–434.
4. Heys KR, Friedrich MG, Truscott RJ. Presbyopia and heat: changes associated with aging of the human lens suggest a functional role for the small heat shock protein, alpha-crystallin, in maintaining lens flexibility. *Aging Cell*. 2007;6:807–815.
5. Pierscionek BK. Age-related response of human lenses to stretching forces. *Exp Eye Res*. 1995;60:325–332.
6. Weeber HA, van der Heijde RG. On the relationship between lens stiffness and accommodative amplitude. *Exp Eye Res*. 2007;85:602–607.
7. Piatigorsky J. Lens differentiation in vertebrates. A review of cellular and molecular features. *Differentiation*. 1981;19:134–153.
8. Bassnett S, Winzenburger PA. Morphometric analysis of fibre cell growth in the developing chicken lens. *Exp Eye Res*. 2003;76:291–302.
9. Kuszak JR. The ultrastructure of epithelial and fiber cells in the crystalline lens. *Int Rev Cytol*. 1995;163:305–350.
10. Koretz JF, Cook CA, Kuszak JR. The zones of discontinuity in the human lens: development and distribution with age. *Vision Res*. 1994;34:2955–2962.
11. Kuszak JR. The development of lens sutures. *Prog Retin Eye Res*. 1995;14:567–591.
12. Cheng C, Nowak RB, Amadeo MB, Biswas SK, Lo WK, Fowler VM. Tropomyosin 3.5 protects the F-actin networks required for tissue biomechanical properties. *J Cell Sci*. 2018;131:jcs222042.
13. Cheng C, Nowak RB, Biswas SK, Lo WK, FitzGerald PG, Fowler VM. Tropomodulin 1 regulation of actin is required for the formation of large paddle protrusions between mature lens fiber cells. *Invest Ophthalmol Vis Sci*. 2016;57:4084–4099.
14. Fudge DS, McCuaig JV, Van Stralen S, et al. Intermediate filaments regulate tissue size and stiffness in the murine lens. *Invest Ophthalmol Vis Sci*. 2011;52:3860–3867.
15. Gokhin DS, Nowak RB, Kim NE, et al. Tmod1 and CP49 synergize to control the fiber cell geometry, transparency, and mechanical stiffness of the mouse lens. *PLoS One*. 2012;7:e48734.
16. Maddala R, Walters M, Brophy PJ, Bennett V, Rao PV. Ankyrin-B directs membrane tethering of periaxin and is required for maintenance of lens fiber cell hexagonal shape and mechanics. *Am J Physiol Cell Physiol*. 2016;310:C115–C126.
17. Sindhu Kumari S, Gupta N, Shiels A, et al. Role of aquaporin 0 in lens biomechanics. *Biochem Biophys Res Commun*. 2015;462:339–345.
18. Parreno J, Cheng C, Nowak RB, Fowler VM. The effects of mechanical strain on mouse eye lens capsule and cellular microstructure. *Mol Biol Cell*. 2018;29:1963–1974.
19. Kullander K, Klein R. Mechanisms and functions of Eph and ephrin signalling. *Nat Rev Mol Cell Biol*. 2002;3:475–486.

20. Arvanitis D, Davy A. Eph/ephrin signaling: networks. *Genes Dev*. 2008;22:416–429.
21. Himanen JP, Saha N, Nikolov DB. Cell-cell signaling via Eph receptors and ephrins. *Curr Opin Cell Biol*. 2007;19:534–542.
22. Davy A, Gale NW, Murray EW, et al. Compartmentalized signaling by GPI-anchored ephrin-A5 requires the Fyn tyrosine kinase to regulate cellular adhesion. *Genes Dev*. 1999;13:3125–3135.
23. Holland SJ, Gale NW, Mbamalu G, Yancopoulos GD, Henkemeyer M, Pawson T. Bidirectional signalling through the EPH-family receptor Nuk and its transmembrane ligands. *Nature*. 1996;383:722–725.
24. Cheng C, Ansari MM, Cooper JA, Gong X. EphA2 and Src regulate equatorial cell morphogenesis during lens development. *Development*. 2013;140:4237–4245.
25. Cheng C, Gong X. Diverse roles of Eph/ephrin signaling in the mouse lens. *PLoS One*. 2011;6:e28147.
26. Jun G, Guo H, Klein BE, et al. *EPHA2* is associated with age-related cortical cataract in mice and humans. *PLoS Genet*. 2009;5:e1000584.
27. Shi Y, De Maria A, Bennett T, Shiels A, Bassnett S. A role for *Epha2* in cell migration and refractive organization of the ocular lens. *Invest Ophthalmol Vis Sci*. 2012;53:551–559.
28. Zhou Y, Shiels A. Epha2 and Efna5 participate in lens cell pattern-formation. *Differentiation*. 2018;102:1–9.
29. Cooper MA, Son AI, Komlos D, Sun Y, Kleiman NJ, Zhou R. Loss of ephrin-A5 function disrupts lens fiber cell packing and leads to cataract. *Proc Natl Acad Sci USA*. 2008;105:16620–16625.
30. Biswas S, Son A, Yu Q, Zhou R, Lo WK. Breakdown of interlocking domains may contribute to formation of membranous globules and lens opacity in ephrin-A5(-/-) mice. *Exp Eye Res*. 2016;145:130–139.
31. Son AI, Cooper MA, Sheleg M, Sun Y, Kleiman NJ, Zhou R. Further analysis of the lens of ephrin-A5-/- mice: development of postnatal defects. *Mol Vis*. 2013;19:254–266.
32. Okabe M, Ikawa M, Kominami K, Nakanishi T, Nishimune Y. 'Green mice' as a source of ubiquitous green cells. *FEBS Lett*. 1997;407:313–319.
33. Frisen J, Yates PA, McLaughlin T, Friedman GC, O'Leary DD, Barbacid M. Ephrin-A5 (AL-1/RAGS) is essential for proper retinal axon guidance and topographic mapping in the mammalian visual system. *Neuron*. 1998;20:235–243.
34. Muzumdar MD, Tasic B, Miyamichi K, Li L, Luo L. A global double-fluorescent Cre reporter mouse. *Genesis*. 2007;45:593–605.
35. Cheng C, Gokhin DS, Nowak RB, Fowler VM. Sequential application of glass coverslips to assess the compressive stiffness of the mouse lens: strain and morphometric analyses. *J Vis Exp*. 2016;111:53986.
36. Baradia H, Nikahd N, Glasser A. Mouse lens stiffness measurements. *Exp Eye Res*. 2010;91:300–307.
37. Cheng C, Parreno J, Nowak RB, et al. Age-related changes in eye lens biomechanics, morphology, refractive index and transparency. *Aging (Albany NY)*. 2019;11:12497–12531.
38. Cheng C, Fowler VM, Gong X. EphA2 and ephrin-A5 are not a receptor-ligand pair in the ocular lens. *Exp Eye Res*. 2017;162:9–17.
39. Lisabeth EM, Falivelli G, Pasquale EB. Eph receptor signaling and ephrins. *Cold Spring Harb Perspect Biol*. 2013;5:a009159.
40. Pasquale EB. Eph-ephrin bidirectional signaling in physiology and disease. *Cell*. 2008;133:38–52.
41. Abdul-Latif ML, Salazar JA, Marshak S, Dinh ML, Cramer KS. Ephrin-A2 and ephrin-A5 guide contralateral targeting but not topographic mapping of ventral cochlear nucleus axons. *Neural Dev*. 2015;10:27.
42. Feldheim DA, Kim YI, Bergemann AD, Frisen J, Barbacid M, Flanagan JG. Genetic analysis of ephrin-A2 and ephrin-A5 shows their requirement in multiple aspects of retinocollicular mapping. *Neuron*. 2000;25:563–574.
43. Wilks TA, Rodger J, Harvey AR. A role for ephrin-As in maintaining topographic organization in register across interconnected central visual pathways. *Eur J Neurosci*. 2010;31:613–622.
44. Sweeney NT, James KN, Sales EC, Feldheim DA. Ephrin-As are required for the topographic mapping but not laminar choice of physiologically distinct RGC types. *Dev Neurobiol*. 2015;75:584–593.
45. Himanen JP. Ectodomain structures of Eph receptors. *Semin Cell Dev Biol*. 2012;23:35–42.
46. Himanen JP, Chumley MJ, Lackmann M, et al. Repelling class discrimination: ephrin-A5 binds to and activates EphB2 receptor signaling. *Nat Neurosci*. 2004;7:501–509.

Supplementary Material

Supplementary Video S1. Lenses from 8-week-old tdTomato+ ephrin-A5+/+ and EphA2+/+ mice. Videos show the z-stack from the anterior epithelial cells into the anterior fibers (~130 µm deep). The cell membranes were fluorescent due to the tdTomato transgene. The lens sutures and apex were well aligned between each shell of fiber cells.

Supplementary Video S2. Lenses from 8-week-old tdTomato+ ephrin-A5+/+ and EphA2+/+ mice. Videos show the z-stack from the anterior epithelial cells into the anterior fibers (~130 µm deep). The cell membranes were fluorescent due to the tdTomato transgene. The lens sutures and apex were well aligned between each shell of fiber cells.

Supplementary Video S3. Lenses from 8-week-old tdTomato+ ephrin-A5−/− and EphA2−/− mice. Videos show the z-stack from the anterior epithelial cells into the anterior fibers (~130 µm deep). The red asterisk marks the apex of the suture in the outer layers of lens fibers, and the green asterisk marks the apex of the suture in the inner layers of fiber cells. Note that the suture apex moved between the different shells of lens fibers.

Supplementary Video S4. Lenses from 8-week-old tdTomato+ ephrin-A5−/− and EphA2−/− mice. Videos show the z-stack from the anterior epithelial cells into the anterior fibers (~130 µm deep). The red asterisk marks the apex of the suture in the outer layers of lens fibers, and the green asterisk marks the apex of the suture in the inner layers of fiber cells. Note that the suture apex moved between the different shells of lens fibers.

Supplementary Video S5. Lenses from 8-week-old tdTomato+ ephrin-A5−/− and EphA2−/− mice. Videos show the z-stack from the anterior epithelial cells into the anterior fibers (~130 µm deep). The < symbols point to extra branches of the Y-suture. Note that the branches often appeared in the outer

Investigative Ophthalmology & Visual Science

shells of lens fibers and disappeared in the inner layers of fiber cells.

Supplementary Video S6. Lenses from 8-week-old tdTomato+ ephrin-A5−/− and EphA2−/− mice. Videos show the z-stack from the anterior epithelial cells into the anterior fibers (~130 µm deep). The < symbols point to extra branches of the Y-suture. Note that the branches often appeared in the outer shells of lens fibers and disappeared in the inner layers of fiber cells.

Investigative Ophthalmology & Visual Science